Miroslav MÜLLER, Zdeněk MÜLLER, Josef TLUSTÝ

Czech Technical University in Prague, Faculty of Electrical Engineering

Overhead Line Mechanical Behaviour - Dynamic Model

Abstract. *The paper presents modelling of overhead line dynamics. The model of overhead line (OHL) shaking is generally based on the superposition of harmonic components. Individual harmonic coordinate components are finally composed together. The accuracy of the calculation is determined by the number of harmonics calculated and other parameters. The model is actually a combination of continuous and discrete calculations. In the case study OHL ACSR 350/59 is analyzed.*

Streszczenie. *W artykule omówiono zagadnienie modelowania dynamicznego linii napowietrznej. Model linii napowietrznej (OHL) jest zasadniczo oparty na superpozycji składowych harmonicznych. Dokładność obliczeń jest określona przez liczbę harmonicznych i inne parametry .Model jest w rzeczywistości kombinacją obliczeń ciągłych i dyskretnych. Szczegółowo przeanalizowano studium przypadku OHL ACSR 350/59* ***(Model dynamiczny zjawisk mechanicznych w linii napowietrznej).***

Słowa kluczowe: linia napowietrzna, dynamiczny model, zjawiska mechaniczne
Keywords: overhead line, dynamic model, mechanical behaviour.

Introduction

The main benefit of using dynamic models consists in evaluation of weather influence depending on its location and time domain. As weather influence may be considered wind force, icing, increased conductor current flow [1], temperature change etc. The dynamic model is, according to its complexity, also useful to simulate various mechanical wave phenomena such as galloping [2, 3, 4]. Usage of models makes characteristic oscillations analysis [5] more accurate and easy. The results contain also stable and unstable spaces around the operating state. The states in the unstable region of the system excitation could result in the wire damage. The described model is a continuous 3-DOF (degrees of freedom) model. A simplified modification of a 2-DOFs model is described in reference [6].

Dynamic model of wire

The analysis of dynamic behaviour is based on the wave equations (1-3). The simulation conditions are depicted in Fig. 1 and 2 - the situation can be taken as a wire strained between two towers. The model is constrained as a string, which can move between the fixed points in horizontal and vertical directions and can also rotate. The possibility of rotation of a wire along its axis is important for simulation with icy wire and is used to solve combined task with icing and wind [7]. This situation is depicted in Fig. 2

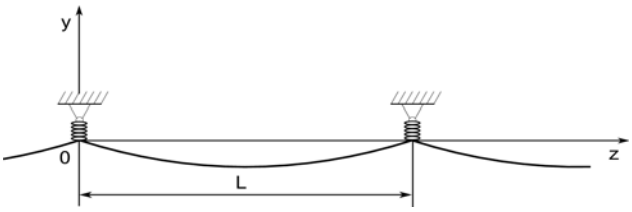

Fig.1. Overhead line field between the towers

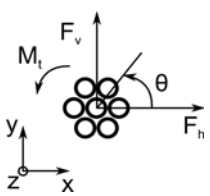

Fig.2. Forces and torque of a force affecting the wire

The dynamics of the wire movement [8, 9] is described by three partial differential equations. The first equation describes the motion of wires in the vertical direction depending on the longitudinal position (variable z) and time t. The second equation describes the wire motion in the horizontal direction. The third equation then adds rotation (torsion) θ. Functions y, x and θ depend on the longitudinal position z and time t.

$$m\frac{\partial^2 y}{\partial t^2}+C_y\frac{\partial y}{\partial t}-T\frac{\partial^2 y}{\partial^2 z}=F_{\mathrm{v}}(z) \tag{1}$$

$$m\frac{\partial^2 x}{\partial t^2}+C_x\frac{\partial x}{\partial t}-T\frac{\partial^2 x}{\partial^2 z}=F_{\mathrm{h}}(z) \tag{2}$$

$$I\frac{\partial^2 \theta}{\partial t^2}+C_\theta\frac{\partial \theta}{\partial t}-GJ\frac{\partial^2 \theta}{\partial^2 z}=M_{\mathrm{t}}(z) \tag{3}$$

where m denotes the mass of wire per 1 m length, I is the moment of inertia, C_y, C_x, C_θ stand for the damping coefficients [10, 11], T is the mechanical stress in the longitudinal direction of the wire, GJ stands for the torsional stress, F_v, F_h are the exciting forces, M_t denotes the torque, and, finally, L denotes the total length of the wire.

The solution of the system of equations strongly depends on the boundary conditions. In our case, the wires at both ends are fixed and thus:

$$x(z=0,t)=y(z=0,t)=\theta(z=0,t)=0 \tag{4}$$

$$x(z=L,t)=y(z=L,t)=\theta(z=L,t)=0 \tag{5}$$

The solving process of the system (1-3) is based on the possibility of separation of variables (with respect to the position and time). This separation is used as a transformation of position by the Fourier transform. This results in a new set of equations for each harmonic:

$$m\frac{\mathrm{d}^2 x_k}{\mathrm{d}t^2}+C_x\frac{\mathrm{d}x_k}{\mathrm{d}t}+T\left(\frac{k\pi}{L}\right)^2 x_k = \\ =\frac{2}{L}\int_0^L F_{\mathrm{v}}(z)\cdot\sin\left(\frac{k\pi z}{L}\right)\mathrm{d}z \tag{6}$$

$$m\frac{\mathrm{d}^2 y_k}{\mathrm{d}t^2}+C_y\frac{\mathrm{d}y_k}{\mathrm{d}t}+T\left(\frac{k\pi}{L}\right)^2 y_k = \\ =\frac{2}{L}\int_0^L F_{\mathrm{h}}(z)\cdot\sin\left(\frac{k\pi z}{L}\right)\mathrm{d}z \tag{7}$$

(8)
$$I\frac{\mathrm{d}^2\theta_k}{\mathrm{d}t^2}+C_\theta\frac{\mathrm{d}\theta_k}{\mathrm{d}t}+GJ\left(\frac{k\pi}{L}\right)^2\theta_k = \\ =\frac{2}{L}\int_0^L M_\mathrm{t}(z)\cdot\sin\left(\frac{k\pi z}{L}\right)\mathrm{d}z$$

The resultant position of the wire is obtained by the superposition of the solutions of equations (6-8) for each calculated harmonics.

Excitation forces

The excitation force model regards the gravitational forces, forces produced by wind blowing and consequent drifting of the wire.

The gravitational force is simulated as a uniform load induced by the gravitational field effects. It is given by the formula

(9) $$F_\mathrm{v}=-mg$$

where g denotes the gravitational constant and m is the weight of the conductor per one meter (including possible ice).

The effect of wind blowing is given by the wire wind resistance. The wire is carried and rotated in this case. The constants describing the relationship between the wire and air are:

(10) $$k_\mathrm{D}=\frac{1}{2}\rho_\mathrm{air}\varphi_\mathrm{cond}$$

(11) $$k_\mathrm{M}=\frac{1}{2}\rho_\mathrm{air}\varphi_\mathrm{cond}^2$$

where ρ_air is the air density and φ_cond denotes the wire diameter.

Wind acting on the wire results in two orthogonal components of the forces. The first one is the force F_D applied in the direction of the wind motion (thus, the main direction). The second one is the component F_L, which is orthogonal to the main direction of blowing. The wire is influenced also by the torque M_ω causing the rotation of both the wire and ice. The positions and orientations, including the actions of forces, are shown in Fig. 3. The figure also includes an ice element. The component forces are described by the set of equations (12–14).

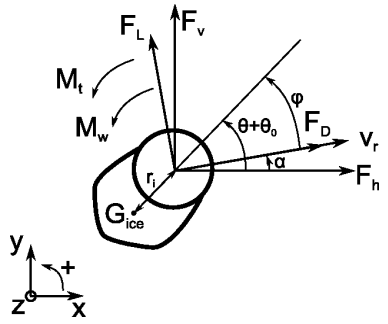

Fig. 3. Wind influence - diagram of angles and forces

(12) $$F_\mathrm{D}=v_\mathrm{r}^2k_\mathrm{D}C_\mathrm{D}(\varphi)$$

(13) $$F_\mathrm{L}=v_\mathrm{r}^2k_\mathrm{D}C_\mathrm{L}(\varphi)$$

(14) $$M_\omega=v_\mathrm{r}^2k_\mathrm{M}C_\mathrm{M}(\varphi)$$

where v_r is the relative wind speed and C_D, C_L, C_M are the transformation functions.

These transformation functions describing the distribution of forces and torque components depend on the directional angle φ. These functions must be obtained from the measurements in an aerodynamic tunnel.

A relative wind speed is another problem to be solved. This speed is calculated as relative, because the wire generally moves, too. The velocity components $v_{\mathrm{r}x}$ and $v_{\mathrm{r}y}$ are given by the formulas

(15) $$v_{\mathrm{r}x}=v_{0x}-\frac{\partial x}{\partial t}-r_\mathrm{i}\frac{\partial\theta}{\partial t}\sin(\theta+\theta_0)$$

(16) $$v_{\mathrm{r}y}=v_{0y}-\frac{\partial y}{\partial t}+r_\mathrm{i}\frac{\partial\theta}{\partial t}\cos(\theta+\theta_0)$$

where x and y are the positions of the conductor, r_i denotes the distance from the centre of gravity of the conductor and centre of gravity of the ice, and θ stands for the rotation of the wire with respect to the rest position θ_0. Now

(17) $$v_\mathrm{r}=\sqrt{v_{\mathrm{r}x}^2+v_{\mathrm{r}y}^2}$$

The angle φ is an important parameter for functions C_D, C_L, C_M. Its value is determined from

(18) $$\tan(\alpha)=\frac{v_{\mathrm{r}x}}{v_{\mathrm{r}y}}$$

(19) $$\varphi=\theta+\theta_0-\alpha-\frac{r_\mathrm{i}}{v_0}\frac{\partial\theta}{\partial t}$$

Since the forces F_D and F_L are described in the system oriented in the direction of the blowing wind and the other equations are in the ground coordinates, it is necessary to transform the results in the directions of F_v and F_h

(20) $$F_\mathrm{v}=F_\mathrm{L}\cos(\alpha)+F_\mathrm{D}\sin(\alpha)-mg$$

(21) $$F_\mathrm{h}=-F_\mathrm{L}\sin(\alpha)+F_\mathrm{D}\cos(\alpha)$$

Case study

The simulations are based on equations described in the previous section. For this case study, simulation of the ACSR 350/59 wire [12] was chosen. Functions C_D, C_L and C_M were taken from [2], because their determination would require a complex technical measuring equipment (aerodynamic tunnel with a tight wire and controlled climatic environment). The span length [13] was set as $a=224$ m and $h\approx 0$ m (the difference in height of the conductor support points). The icing of the wire was 0.6 kg/m and tension was assumed $T=35600$ N.

Basic simulation

The simulation shows the step response of the new wire under the constant influence of wind speed $\boldsymbol{v}_0=(16, 5.2)$ m condition (relative angle position of icing is assumed to be steady). During the calculation only odd harmonics were taken into account (within the range from the first to seventh harmonics). Even harmonics are zero functions in this case.

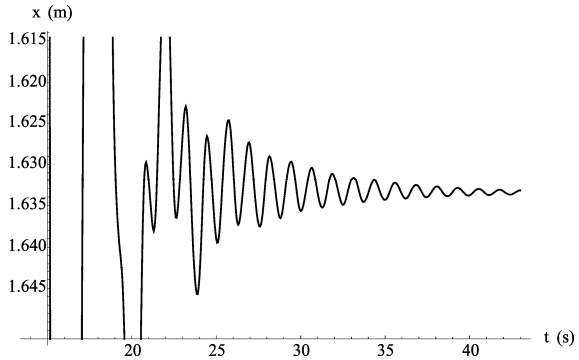

Fig. 4. x -coordinates in the middle of wire span ($z = L/2$).

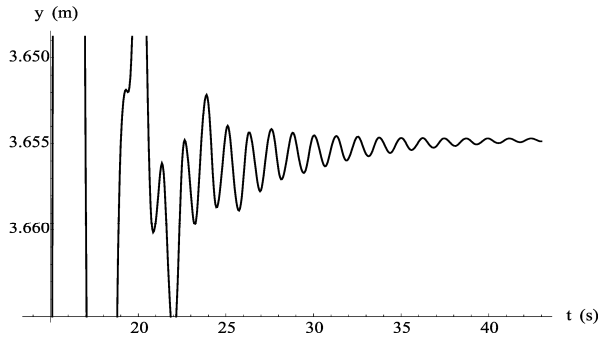

Fig. 5. y -coordinates in the middle of wire span ($z = L/2$).

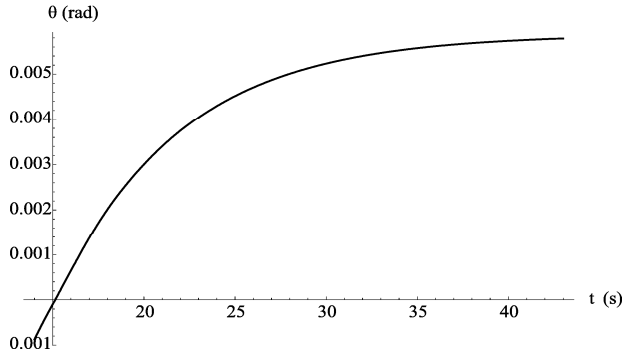

Fig. 6. Rotation of the wire θ in the middle of the wire span ($z = L/2$)

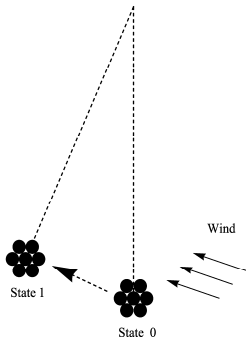

Fig. 7 Schematic representation of wire movement due to wind influence.

Figures 4–6 show wire positions for $z = L/2$ (the middle of the wire span) in time. Since the wire is influenced by constant wind blow v_0 and system is in stable state, the position of the wire results in the stable equilibrium. Schematically the situation is shown in Fig. 7 where "State 0" is the steady equilibrium for the state without wind and "State 1" is the stable position with the influence of a constant wind of velocity v_0. Coordinate y contains gravitational forces causing an offset.

For determining the position of each coordinate it is necessary to evaluate a few harmonics (6-8) for each component. Sub-harmonics results are shown in Figs. 8–10. Since the conductor own load is constant and other parameters are also homogenous (including icing), the solutions do not contain even harmonics. This fact results in a simplification of the calculations and even harmonics have not to be taken into account. In the case of a non-constant load, this simplifying assumption does not generally apply.

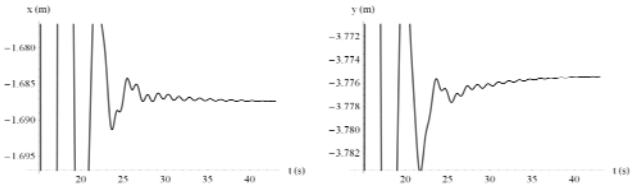

Fig. 8. The first harmonic amplitudes of position in time

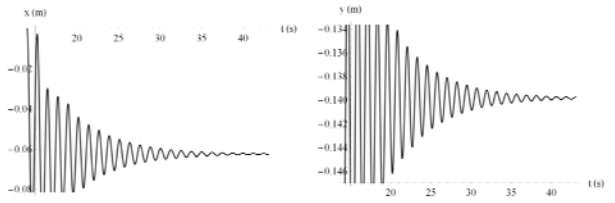

Fig. 9. The third harmonic amplitudes of position in time

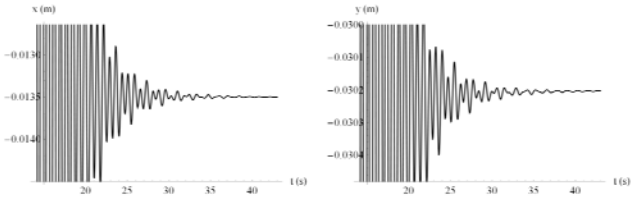

Fig. 10. The fifth harmonic amplitudes of position in time

Effect of icing position

The following simulation is done under the same conditions as above. The only change is in the variation of icing position angle θ_0 (see Fig. 3). The results for the steady state are listed in Table. 1. The values in the table show that icing created under windy conditions leads to really different results than in case of homogeneous conditions.

Table 1. Steady state value for different angle θ_0

θ_0	$x\ (z = L/2)$	$y\ (z = L/2)$	$\theta\ (z = L/2)$
(°)	(m)	(m)	(°)
18.000	-1.199	-3.819	0.007
0.000	-1.355	-3.891	22.074
-18.000	-1.619	-3.677	20.375
-36.000	-1.877	-3.250	-15.042
-54.000	-2.079	-2.895	-78.379

Influence of calculated harmonics on simulation results

The influence of harmonic components taking into account the calculated steady state is shown in Table 2. The influence of harmonics is determined by repeated calculations throughout the simulation by reducing the number of harmonics in the calculation. This is not only the decomposition of the resulting values in the steady state. A

simple decomposition cannot be used because it is a nonlinear system.

Table 2. Steady state value harmonics taken account

Harmonic order	$x\ (z = L/2)$	$y\ (z = L/2)$	$\theta\ (z = L/2)$
(-)	(m)	(m)	(°)
1	-1.6876	-3.7751	0.00617
3	-1.6249	-3.6355	0.00585
5	-1.6385	-3.6657	0.00589
7	-1.6336	-3.6547	0.00588
9	-1.6359	-3.6598	0.00588

The values show that with the growing order of harmonics there decreases its influence on the results. Effect of the ninth and higher harmonics is then low, and their added value in comparison with the complexity of the calculation is negligible.

Conclusion

This paper describes a 3-DOF model for modeling of the dynamic behaviour of a stretched wire. The main outer influences on the model have been described. Furthermore, the wind effect on the conductor with icing has been described.

In the basic case study it has been shown a wire with constant icy and wind blow. In the case study simulations show the position of the middle of the span for all 3 coordinates. Furthermore, the behavior of each harmonics is calculated. The time evolution of displacements x, y, θ depending on the coordinate z can be viewed for other locations, but it does not take importance for this distribution of the forces. In this part it has also been studied the influence of turning of the frozen wire. From the simulation it is clearly visible that the wire with significant icing placed in one direction (center of gravity is shifted from the center of wire) is very sensible on wind parameters (Tab. 1). In the real situation, icing is placed asymmetrically. In this case it is possible to choose a characteristic direction and use an average value. For more accurate results it would be necessary to describe the distribution function for icing including the directional angle and shift of gravity along the wire length z.

As a part of the study the influence of the number of solved equations was calculated, where one set of 3 equations represents one harmonic. From this simulation and from the model it can be deduced that the even harmonics do not affect the solution for uniform distribution of forces and weight. Furthermore, the influence of the ninth and higher harmonics is for simulation negligible compared with the complexity of calculation.

Financial support of the Ministry of Education, Youth and Sports, through grant number MSM 6840770017, is highly acknowledged.

REFERENCES

[1] Toman, P., Paar, M.; Orságová, J. Possible Solutions to Problems of Voltage Asymmetry and Localization of Failures in MV Compensated Networks. In 2007 *IEEE Lausanne Powertech*, Vol 1-5.1., Lausanne: Ecole Polytechnique Federale de Lausanne, 2007. pp. 1758-1763. ISBN: 978-1-4244-2189-3.

[2] Lilien, J. L. Overhead Line Vertical Galloping on Bundle Configurations: Stability Criterions and Amplitude Prediction, Overhead Line Design and Construction: Theory and Practice, 1989., *International Conference, London UK*, pp. 65-69.

[3] Sergey, J., Klimkowicz, P., Kozak, C., Influence of moving single conductors and detuning pendulums on parameters of galloping energy-transmission lines, *Przegląd elektrotechniczny*. 2010, Vol. 86, No. 7, pp. 154-156.

[4] Chan, J., et al. EPRI Transmission Line Refernce Book: Wind - Induced Conductor Motion, 2006, EPRI, Palo Alto

[5] Claren, R., Diana, G. Mathematical Analysis of Transmission Line Vibration, *IEEE Transactions on Power Apparatus and Systems*, Vol. Pas-88, No. 12, December 1969, pp. 1741-1771.

[6] Wang, J., Lilien, J.L. Overhead Transmission Line Galloping. A Comparative Study between 2-DOF and 3-DOF Models., c1994, *3ème Congrès National Belge de Mécanique Théorique et Appliquée. Liège*, May. Actes du 3ème CNBM. pp. 257-260.

[7] Simpson, A., Wind-induced Vibration of Overhead Power Transmission Lines, Sci. Prog. Oxford 68, pp.285-308, 1983.

[8] Wang, J., Lilien, J. L. Overhead Electrical Transmission Line Galloping - A Full Multi-Span 3-DOF Model, Some Applications and Design Recommendations, *IEEE Transactions on Power Delivery*, Vol. 13, No. 3, July 1998, pp. 909-916.

[9] Lilien, J. L., Wang, J., Chabart, O., Pirotte, P. Overhead Transmission Lines Design Some Mechanical Aspects, 1994, *ICPST'94 (International Conference on Power System Technology)*. October 18-21. Beijing, China. 5 pages.

[10] Rawlins, C. B. An Efficient Method for Measuring Dissipation by Dampers in Laboratory Spans, *IEEE Transactions on Power Delivery*, Vol. 3, No. 3, July 1988, pp. 1146-1156.

[11] Rawlins, C. B. An Efficient Method for Measuring by Dampers in Laboratory Spans, *IEEE Transactions on Power Delivery*, Vol. 3, No. 3, July 1988, pp. 1146-1156.

[12] Lanové vodice, Žiar nad Hronom: [ŽHS], 2007, <http://www.lana.sk> (08.03.2012)

[13] Kiessling, F., Nefzger, P., Nolasco, J. F., Kaintzyk, U. Overhead Power Lines - Planning, Design, Construction, Germany: Springer, 2003, ISBN 3-540-00297-9.

***Authors**: dr. inż. Miroslav Müller, Czech Technical University in Prague, Technická 2, 166 27 Prague 6, Czech Republic; E-mail: miroslav.muller@fel.cvut.cz; dr. inż. Zdeněk Müller, Czech Technical University in Prague, Technická 2, 166 27 Prague 6, Czech Republic; E-mail: zdenek.muller@fel.cvut.cz; prof. dr inż. Josef Tlustý, Czech Technical University in Prague, Technická 2, 166 27 Prague 6, Czech Republic; E-mail: tlusty@fel.cvut.cz.*